A theoretical examination of the molecular packing, intermolecular bonding and crystal morphology of 2,4,6-trinitrotoluene in relation to polymorphic structural stability

Hugh G. Gallagher,[a] Kevin J. Roberts,[b] John N. Sherwood[c] and Lorna A. Smith[d]

[a] *Department of Physics and Applied Physics, University of Strathclyde, Glasgow, UK G1 1XL*
[b] *Centre for Molecular and Interface Engineering, Department of Mechanical and Chemical Engineering, Heriot-Watt University, Edinburgh, UK EH14 4AS*
[c] *Department of Pure and Applied Chemistry, University of Strathclyde, Glasgow, UK G1 1XL*
[d] *Department of Pure and Applied Chemistry, University of Strathclyde, Glasgow, G1 1XL and Centre for Molecular and Interface Engineering, Department of Mechanical and Chemical Engineering, Heriot-Watt University, Edinburgh, UK EH14 4AS*

2,4,6-Trinitrotoluene (TNT) can crystallise in both monoclinic and orthorhombic polymorphic forms characterised by two distinct molecular packing configurations in the solid-state associated with two conformationally unique molecules (A and B) in the asymmetric unit with four asymmetric units in the unit cell. In this the centrosymmetric monoclinic (pseudo *b*-glide) structure ($P2_1/c$) adopts an AABBAABB packing motif and the orthorhombic (pseudo-centrosymmetric structure $Pb2_1a$) adopts an ABABABAB packing motif. The close molecular similarity between the conformations of the A and B molecules also gives rise to twinning in the monoclinic phase due to defects in the stacking sequence. The two molecular structures differ in the degree to which the 2,4,6 nitro groups are twisted out of the plane of the benzene ring and there are also subtle differences in the molecular conformation of the two molecular types between the two polymorphs. Lattice energy calculations based on the solved structures reflect the similarity of the packing sequences, suggesting a relative stability of monoclinic > twinned monoclinic > orthorhombic in agreement with experimental studies. The small energy difference between the twinned and non-twinned monoclinic polymorphs explains the abundance of twinning in TNT. Attachment energy calculations predict needle-like crystal morphologies with a plate-like cross-section.

Polymorphism plays a major role in the performance, production and long-term stability of many chemical and biochemical products. The polymorphic form of a material can affect a wide range of physical, chemical and biochemical properties,[1–3] including density, hardness, ductility and colour, solid-state reactivity and bioavailability. Studies of the structural aspects of polymorphism have been carried out by a number of workers,[4–6] *e.g.* on 1,4-dichlorobenzene,[7] *o*-acetamidobenzamide[8] and benzylideneaniline.[9–12] Crystallographic analyses, *via* studies of molecular conformation and packing motif, have been found to be invaluable in elucidating the nature and transformation mechanisms associated with polymorphic behaviour in the organic solid state.

The crystallisation behaviour of TNT has been the subject of considerable attention since the late eighteenth century when various authors[13–19] observed orthorhombic and monoclinic polymorphs as well as numerous variants of the two modifications depending on the method of preparation. More recently Gallagher and Sherwood[20–22] systematically investigated the structural nature, relative stability and morphology of TNT crystals grown from solution. Three basic forms were found to exist with monoclinic, orthorhombic and twinned monoclinic structures respectively. Subsequent examination revealed the monoclinic polymorph to be the thermodynamically more stable form under ambient conditions. A model of the twinned monoclinic structure was presented which attributed the predominance of twinning to the presence of pseudo-symmetry elements between successive molecular layers in the packing arrangement of the monoclinic form. Variations in both structure and morphology with growth conditions were observed.

In this paper molecular and crystallographic modelling techniques have been used to examine in detail the crystal structures of the polymorphic forms with a view to rationalising the experimental data of Gallagher and Sherwood in terms of the packing energetics and hence relative stability of the two structures. Lattice energy calculations have also been performed on the previously proposed model[20–22] of the twinned structure and have been used to explain the energetic basis for the observed twinning. In addition, predictions of the morphologically important crystal faces have been made in order to understand the observed variation in morphology with different growth conditions.

Computational methods

Structural parameters

The structural coordinates for the monoclinic and orthorhombic forms were determined by Duke[14] and are given in supplementary material.† The monoclinic form has the space group $P2_1/c$ and unit-cell dimensions $a = 21.275$ Å, $b = 6.093$ Å, $c = 15.025$ Å, $\beta = 110.23°$. The orthorhombic form has the space group $Pb2_1a$ and unit-cell dimensions $a = 15.075$ Å, $b = 20.024$ Å and $c = 6.107$ Å. As no structural data existed for the twinned crystal the molecular arrangement about the twin fault was generated by imbedding a unit cell of the orthorhombic polymorph within the monoclinic structure using the modelling system INTERCHEM[23] and the program CRYSTLINK.[24] Within HABIT95[29–31] these coordinates were generated repeatedly along the twin fault direction whilst monoclinic unit cells were stacked repeatedly above and below

---

† Deposited at the British Library: SUP **57198** (5 pp.). Details available from the Editorial Office.

the twin fault. The atomic coordinators for all these structures are also given in the supplementary material.†

Calculation of the intermolecular interactions, lattice energy and the crystal morphology

Using the atom–atom method,[25] the strength of an intermolecular interaction can be approximated to a summation of all the constituent atom–atom interactions between the two molecules. The lattice energy is simply the summation of all the intermolecular forces in the crystal lattice. For a central molecule (with n atoms) surrounded by N molecules (each containing n' atoms) the lattice energy can be given by:

$$E=\frac{1}{2}\sum_{k=1}^{N}\sum_{i=1}^{n}\sum_{j=1}^{n'}V_{k_{ij}}$$

where $V_{k_{ij}}$ is the interaction energy between atom i of the central molecule and j of the kth surrounding molecule, with the factor 1/2 reflecting the summed total coming from a pair of interactions.

The atom–atom interactions were calculated using the parameter set of Scheraga *et al.*[26] which was derived for hydrocarbons, carboxylic acids and amides and has been shown to give accurate results for these systems. The partial atomic charges of each molecule were calculated using the self-consistent force-field MNDO[27] (modified neglect of differential overlap) method within MOPAC[28] with the actual values given in the supplementary material.†

The intermolecular bond strengths and resulting lattice energies were calculated using the program HABIT95.[29–31] The program identifies the atom–atom pairs between a central molecule and all the surrounding molecules within a sphere and evaluates their interaction energies.

The validity of the intermolecular force-field was assessed with respect to thermodynamic parameters *via* the calculation of the experimental sublimation enthalpy[32,33] (V_{exp}) which is related to the sublimation enthalpy ($\Delta_{\mathrm{sub}}H$) by the equation:

$$V_{\mathrm{exp}}=-\Delta_{\mathrm{sub}}H-2RT$$

where V_{exp} is the lattice energy, $\Delta_{\mathrm{sub}}H$ is the enthalpy of sublimation and $2RT$ represents a correction factor for the difference between the gas-phase enthalpy and the vibrational contribution to the crystal enthalpy.[34] The accuracy of the calculations depends upon the force-field utilised, a reasonable error being ± 0.25 kcal mol^{-1} (1 cal = 4.184 J). Despite this, lattice energy calculations usually provide a reliable method of predicting the order of thermodynamic stability of a series of systems.[4,7]

The crystal morphology was predicted *via* an attachment energy (E_{att}) calculation where E_{att} is the fraction of the total lattice energy released on the attachment of a slice to a growing crystal surface. HABIT95[29–31] calculates the attachment energy of suitable slices by summing the individual interactions between the central molecule and all the molecules outwith a slice of thickness d_{hkl}, but within the limiting sphere radius. Suitable slices (hkl) for these calculations were obtained using a Bravais–Freidel–Donnay–Harker[35–38] analysis *via* the computer program MORANG.[24]

Results and Discussion

Molecular conformation

Examination of the crystal structures determined by Duke[14] reveals a similarity between the orthorhombic and monoclinic polymorphs in both their packing and in their molecular configurations. The TNT molecules in both the orthorhombic and monoclinic polymorphs exist in two unique conformational forms, A and B. Both structures have four asymmetric units in the unit cell, each containing one type A and one type B molecule. The monoclinic polymorph has a pseudo b-glide plane with a real centre of symmetry whilst the orthorhombic polymorph has a real b-glide plane and a pseudo-centrosymmetric structure. The A and B type molecules of the monoclinic form are stacked in the sequence AABBAABB perpendicular to the bc plane, while the orthorhombic form has a stacking sequence of ABABABAB parallel to the b axis. These pseudo-elements cause the packing differences between the two polymorphs to be small.

Fig. 1 shows the intramolecular interaction distances and angles for the A and B type molecules of both the monoclinic and orthorhombic polymorphs. The interior angles of the carbon atoms attached to the nitro groups are all greater than 120° in both polymorphs, reflecting distortion of the benzene rings. The nitro groups in both polymorphs form non-zero dihedral angles with the plane of the benzene ring. In the monoclinic polymorph the 2,4,6 nitro groups are twisted out of the plane by 59.4, 32.2 and 40.1° for the A form and by 49.9, 22.2 and 46.1° for the B form. For the orthorhombic polymorph they are twisted out of the plane by 58.8, 32.2 and 41.3° for the A form and by 50.1, 21.7 and 45.7° for the B form. A similar twisting has been found in both 2,4,6-trinitroaniline[38] and 2,3,4,6-tetranitroaniline[39] where it was argued that it was a result of crowding between groups. This crowding is reflected in the high densities of these species (1.762 g cm^{-3} for trinitroaniline and only 1.87 g cm^{-3} for tetranitroaniline) and hence this argument can be extended to both the monoclinic and orthorhombic forms of TNT which also exhibit high densities (1.650 g cm^{-3} and 1.645 g cm^{-3} respectively). These observations are in agreement with those of Carper *et al.*[40] for orthorhombic TNT. The extent to which the nitro groups twist out of the plane of the benzene ring is similar for both the A type molecules of the different polymorphs and for both the B type molecules. The twisting is, however, considerably different between molecules of type A and B within the same polymorph. Root-mean-square fit values have been calculated using INTERCHEM and are reported in Table 1. Values are calculated between similar types of molecules in different polymorphs and between different types of molecules within the same polymorph. These values emphasise the greater similarity of the A type molecules of both polymorphs and of the B type molecules of both polymorphs in comparison to A and B type molecules of the same polymorph. The similarity between the molecules of different polymorphs emphasises the conformational similarity of the two polymorphs.

Molecular packing in the crystal structure

The monoclinic structure consists of pairs of identical molecules related by symmetry centres arranged in layers perpendicular to the bc plane. The centres of symmetry occur at positions (0,0,1/2) and (0,1/2,0) for molecules of type B and at (1/2,0,1/2) and (1/2,1/2,0) for molecules of type A. The layers are linked by a pseudo-glide plane. Fig. 2 shows a projection of the (001) plane of the orthorhombic polymorph. In the orthorhombic polymorph the layers contain pairs of the two A and B forms. These are related by pseudo-centres of symmetry at the approximate coordinates (23/8,0,1/4). A true glide plane, parallel to the b axis, exists between successive layers. Fig. 3 shows a projection of the (010) plane of the monoclinic polymorph.

In both polymorphs hydrogen bonds of the type C—H···O exist. In the case of the orthorhombic polymorph seven hydrogen bonds occur, three of these being of the type B···B, two of the type A···A and two of the type A···B. Table 2 gives the calculated strengths of these intermolecular bonding interactions. The B···B type bonds are weaker than the A···A bonds and the A···B bonds are weaker than both. The monoclinic polymorph has two A···A type bonds, one B···B type

---

† See footnote on previous page.

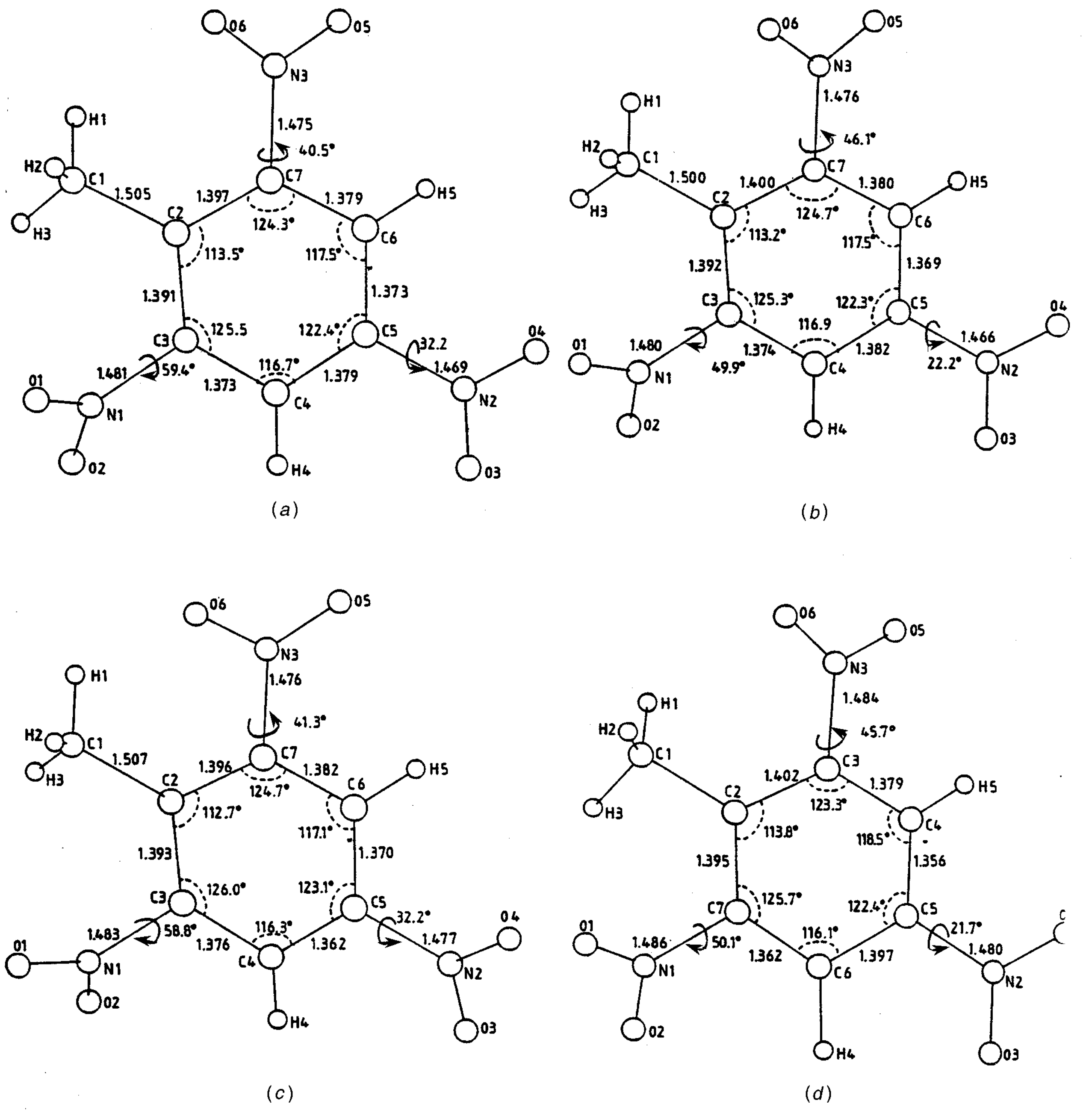

Fig. 1 (*a*) Molecular form A of monoclinic TNT, (*b*) molecular form B of monoclinic TNT, (*c*) molecular form A of orthorhombic TNT and (*d*) molecular form B of orthorhombic TNT

Table 1 Root-mean-square fit values for TNT polymorph molecules overlaid

molecule 1	molecule 2	rms fit/Å
monoclinic, molecule A	orthorhombic, molecule A	0.0969
monoclinic, molecule A	monoclinic, molecule B	0.1427
monoclinic, molecule B	orthorhombic, molecule B	0.0828
orthorhombic, molecule A	orthorhombic, molecule B	0.1790

bond and two A···B type bonds. The strengths of all these bonds are fairly similar, with the exception of one weak A···A type bond.

Group–subgroup relationship between the two polymorphic forms

Examination of the two space groups ($P2_1/c$ and $Pb2_1a$) reveals the two polymorphic structures not to be related by a group–subgroup relationship. The phase transformation between these involves the loss of one symmetry element and the addition of another. Hence this must involve a first-order process and is likely to be a rather disruptive event. A pure solid–solid phase transformation can thus not take place, with the phase transformation likely to involve the complete dissolution of the first form followed by the regrowth of the second. Given the energetic nature of the material the implication of such a disruption is important. The similarity of the two molecular forms (A and B) gives rise to good correspondence between the two structural modifications. If the two structures were superimposed in space the first two layers would coincide almost exactly, while the second two would be displaced relative to one another by $c/2$ with respect to the monoclinic axis system, repeated throughout the structure.

Both polymorphs can be regarded as being related to the same mother-phase *Pbma*, *i.e.* to a phase containing both the suppressed symmetry elements. Whilst there is no evidence for

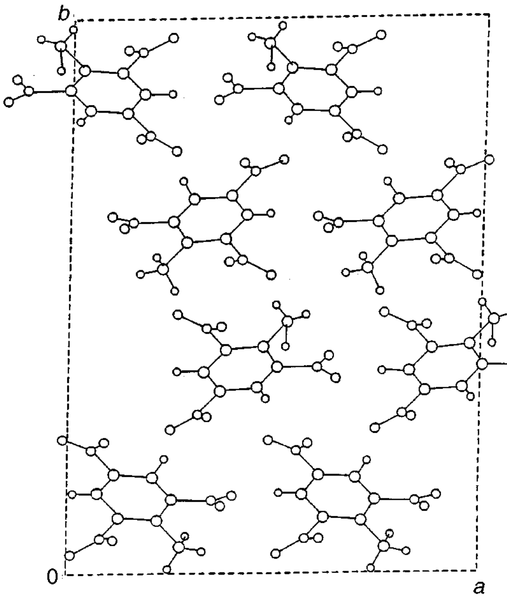

Fig. 2 Projection of the 001 plane of the orthorhombic polymorphic phase of TNT

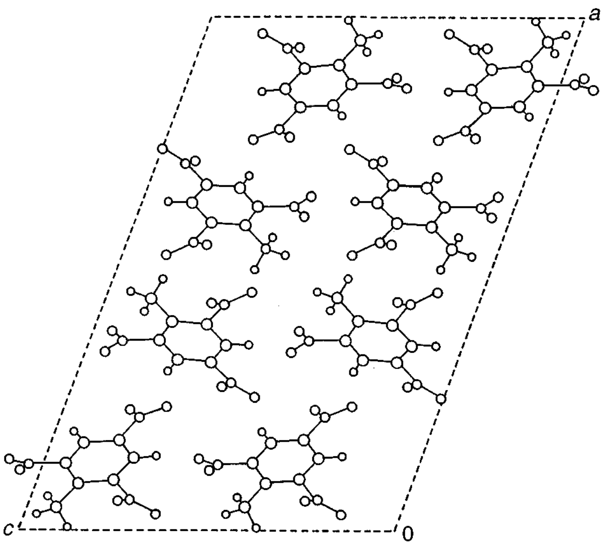

Fig. 3 Projection of the 010 plane of the monoclinic polymorphic phase of TNT

Table 2 Intermolecular interactions for both the monoclinic and orthorhombic polymorphs

	orthorhombic		monoclinic	
type	length/Å	strength/ kcal mol^{-1}	length/Å	strength/ kcal mol^{-1}
A···A	2.60	−1.428	2.59	−0.244
A···A	2.99	−0.949	2.72	−0.911
B···B	2.75	−0.799	2.66	−0.920
B···B	2.60	−0.315	—	—
B···B	2.98	−0.828	—	—
A···B	2.73	−0.429	2.54	−0.887
A···B	2.73	−0.166	2.77	−0.953

the formation of this phase under ambient conditions prior to melting it can be speculated that such a phase might be observed at higher pressures and that this might be reflected in the energetic nature of such a phase.

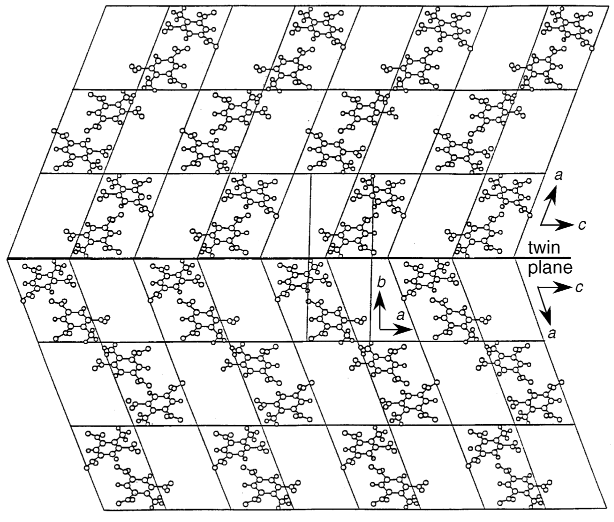

Fig. 4 Crystal packing diagram showing generation of 180° twin plane in the monoclinic (stacking sequence AABBAA) polymorphic form of TNT associated with the embedding of an orthorhombic unit cell (stacking sequence ABAB) on the twin plane boundary

Twinning in the monoclinic phase

Twinning in monoclinic TNT has been identified by Gallagher and Sherwood,[22] who also proposed a model for the twinned structure. In the monoclinic phase, the pseudo-glide plane relates alternate molecular layers perpendicular to the *bc* plane. During crystallisation, this element of pseudo-symmetry can promote deviation from the normal stacking sequence, corresponding to a relatively minor conformational change in the molecules of the faulted layer. Subsequent layers continue in the normal sequence, although they are displaced in a symmetrically related direction. This produces a twin fault within the crystal as shown in Fig. 4. The regions above and below the twin plane follow the usual monoclinic stacking sequence, although they are now related to each other by an angle of 180° around an axis perpendicular to the {100} plane. The new stacking sequence across the boundary corresponds to the orthorhombic structure.

The nature of the twinning creates an orthorhombic cell (ABAB stacking sequence) within a monoclinic structure (*i.e.* A+AABBAABB→A+ABAB+AABB, *etc.*). This causes a switch in the stacking sequence with A molecules either side of the orthorhombic cell which can be regarded as a 180° rotation about an axis perpendicular to the (100) plane.

Calculation of the strength of the intermolecular interactions and lattice energy

Lattice energy convergence was reached *via* summing the intermolecular interaction to a limit of 30 Å for both polymorphs. The lattice energies were calculated using both the A and B molecules as the origin molecule and then averaged. The lattice energies of the A and B molecules were −29.01 and −28.56 kcal mol^{-1} respectively for the monoclinic polymorph and −28.29 and −28.18 kcal mol^{-1} respectively for the orthorhombic polymorph. These variations reflect the different atomic positions for the A and B molecules in the two polymorphs. The calculated lattice energy of the monoclinic polymorph is −28.83 kcal mol^{-1}, and that of the orthorhombic polymorph is −28.24 kcal mol^{-1}. These values are in good agreement with the sublimation enthalpy ($-2RT$) of 28.3±1.0 kcal mol^{-1} reported by Edwards[41] and compare well with that reported by Lenchitz and Velidly[42] (24.7 kcal mol^{-1}). The similarity between the lattice energies reflects the similarity between the crystal structures. The fact that the monoclinic polymorph has a slightly more negative lattice energy suggests it is the most stable, confirming the previous experimental observations.[20–22] The difference in the lattice energies of the two polymorphic forms, 0.59 kcal mol^{-1}, represents the energy of transformation from the monoclinic to the orthorhombic polymorph. This can be compared to the two reported experimental values of $\Delta_{tr}H = 0.22$ kcal mol^{-1} [22] and $\Delta_{tr}H = 0.27 \pm 0.07$ kcal mol^{-1}.[43] The discrepancy between the experimental and calculated values may be accounted for by the presence of twinning or crystallographic impurities in the samples.

The average lattice energy for the twinned structure was calculated as -28.43 kcal mol^{-1}, with a lattice energy of -28.57 kcal mol^{-1} calculated using molecule A as the origin molecule and a lattice energy of -28.28 kcal mol^{-1} using molecule B as the origin molecule.

The small difference in the lattice energy of the twinned crystal and the monoclinic polymorph explains the abundance of twin faults in TNT crystals. As a consequence of the small energy difference, the crystallisation conditions become increasingly important so that minor variations in growth rate or the presence of impurities may result in the occurrence of twinning. For example, under unstable growth conditions it is highly likely that the molecular selectivity needed to differentiate between type A and B molecules in order to achieve a strict monoclinic AABBAA packing might not always be achieved.

Table 3 give the major types and strengths of the intermolecular bonds involved in the monoclinic, orthorhombic and twinned polymorphs. The bond strengths are average values, taken by summing all the constituent atom–atom interactions. Slight variations exist in the strength of the intermolecular interactions for the same type of bonds, *i.e.* A···A, A···B and B···B, along different directions. Both the monoclinic and orthorhombic polymorphs are dominated by eight types of intermolecular interactions, accounting for 87.95 and 88.22% respectively of the total lattice energy. The similarity between the strengths of these bonds reflects the similarity in conformation and packing motif between the two polymorphs. The twinned crystal exhibits eight intermolecular bonds, similar in nature and strength to those in the monoclinic polymorph.

Morphological prediction

Table 4 shows the attachment energies and associated *d*-spacings for the most morphologically important faces together with the percentage of the surface area for the three polymorphs. Fig. 5 shows the resulting predicted morphologies.

For the monoclinic polymorph, a plate-like habit dominated by the {100} face is predicted. The plate-like habit suggests that the monoclinic polymorph crystallises in a layer-like structure in which the bonding between adjacent {100} layers is considerably weaker in comparison to the bonding interactions contained within the layers. Examination of the intermolecular bonds confirms this observation with all the principal intermolecular interactions ($M_a \cdots M_h$) being involved within the slice and none perpendicular to the slice. The resulting small attachment energy of the {100} layers causes slow growth perpendicular to the {100} face. Rapid growth occurs perpendicular to the {110}, {1–1–1} and {011} faces, owing to the presence of strong intermolecular interactions parallel to the *b* axis associated with the strong type M_a, M_b and M_d interactions which link these chains ($4M_a + 2M_b + M_d$). The resulting bonding network creates a series of strong bonding chains, leading to rapid growth, perpendicular to faces {110}, {1−1−1} and {011}. These observations are consistent with the experimental observation that perfect cleavage occurs readily parallel to these planes.[22]

A similar situation occurs for the orthorhombic polymorph, where a plate-like habit dominated by the {010} is predicted. The dominance of the {010} face is due to all the principal intermolecular interactions being involved in bonding within

Table 3 Type and strengths of the intermolecular interactions of the monoclinic, orthorhombic and twinned polymorphs

					interaction energy/ (kcal mol^{-1})		
interactions[a]	*I J U V W Z J*[b]	type[c]	no. of bonds	distance[d]/Å	Coulombic	total	% total energy
M_a	1 1 0 −1 0 1 1	like	2	6.1	−0.49	−2.83	19.6
M_b	1 2 0 0 0 2 2	like	2	6.2	−0.29	−2.76	19.2
M_c	2 1 0 1 0 2 2	unlike	1	6.0	−0.40	−2.71	9.4
M_d	2 1 0 2 1 3 2	unlike	1	6.9	−0.63	−2.60	9.0
M_e	2 1 0 3 0 3 1	like	2	8.1	−0.29	−1.67	11.6
M_f	4 1 0 −1 1 1 1	like	2	8.1	−0.26	−1.49	10.3
M_g	2 1 −1 2 −1 4 1	like	1	8.0	−0.16	−1.37	4.7
M_h	4 1 0 −2 0 4 2	unlike	1	8.5	−0.20	−1.17	4.1
O_a	2 1 0 0 1 2 1	like	2	6.1	−0.42	−2.61	18.5
O_b	1 1 0 0 0 2 2	unlike	2	6.2	−0.31	−2.75	19.5
O_c	2 1 0 0 0 2 2	unlike	1	6.1	−0.44	−2.74	9.7
O_d	4 1 1 0 1 2 2	unlike	1	6.9	−0.65	−2.64	9.3
O_e	2 1 −1 0 −1 4 1	like	2	8.1	−0.31	−1.68	11.9
O_f	4 1 0 0 0 2 1	like	2	8.1	−0.25	−1.48	10.5
O_g	2 1 −1 1 0 3 2	unlike	1	8.0	−0.17	−1.33	4.7
O_h	2 1 0 0 −1 2 2	unlike	1	8.6	−0.17	−1.18	4.2
T_a	1 5 0 −1 0 1 5	like	2	9.09	−0.48	−2.80	19.71
T_b	1 4 0 1 0 1 6	unlike	2	6.17	−0.30	−2.77	19.47
T_c	1 1 0 −1 0 1 3	unlike	1	6.04	−0.41	−2.58	9.07
T_d	1 4 0 0 0 1 1	unlike	1	6.89	−0.64	−2.41	8.46
T_e	1 7 0 −1 −1 1 8	like	2	8.09	−0.29	−1.66	11.64
T_f	1 6 0 0 0 1 5	like	2	8.13	−0.32	−1.55	10.90
T_g	1 2 −1 0 1 1 7	unlike	1	7.99	−0.15	−1.37	4.82
T_h	1 1 0 −2 0 1 3	unlike	1	8.54	−0.22	−1.18	4.17

[a] M_x, O_x and T_x represents monoclinic, orthorhombic and twinned bonds respectively. [b] *I* and *J* refer to the asymmetric unit and molecule representing the origin, while *Z* and *J* represent the asymmetric unit and molecule of the other molecule. *UVW* represent the unit-cell vector. The origin vector is 000. [c] This refers to the nature of the bond. A bond labelled 'like' is a bond between either all A type molecules or all B type molecules. A bond labelled 'unlike' refers to an interaction between both A and B bonds. [d] This refers to the distance between the centres of gravity of the two independent molecules.

Table 4 Slice shift, attachment energies, *d*-spacing and % area of the crystal for the growth faces of the monoclinic, orthorhombic and twinned polymorphs

polymorph	growth face	slice shift/Å	E_{att}/kcal mol^{-1}	*d*-spacing	% area
monoclinic	{1 0 0}	0.0	0.40	20.0	44.7
monoclinic	{0 0 1}	1.4	4.39	14.1	2.4
monoclinic	{1 0 −1}	1.4	4.41	14.0	1.7
monoclinic	{1 1 0}	0.3	16.53	5.8	0.4
monoclinic	{1 −1 −1}	0.6	16.94	5.6	0.1
monoclinic	{0 1 1}	0.8	16.95	5.6	0.1
monoclinic	{1 0 −2}	0.0	13.08	7.5	—
monoclinic	{1 0 2}	0.0	15.09	6.0	—
monoclinic	{1 1 1}	1.6	16.96	5.2	—
orthorhombic	{0 1 0}	1.0	0.40	20.0	44.3
orthorhombic	{1 0 0}	0.8	3.91	15.0	4.6
orthorhombic	{0 1 −1}	0.3	16.01	5.8	0.6
orthorhombic	{1 1 0}	0.6	6.77	12.0	—
orthorhombic	{2 1 0}	0.0	13.03	7.0	—
orthorhombic	{2 1 −2}	0.3	21.63	2.8	—
twinned	{1 0 0}	0.0	−0.40	20.0	44.7
twinned	{0 0 1}	−1.4	−4.40	14.1	2.4
twinned	{1 0 −1}	1.4	−4.41	14.0	1.8
twinned	{1 1 0}	0.6	−16.4	5.8	0.9
twinned	{1 −1 −1}	−0.6	−16.8	5.6	0.1
twinned	{0 1 1}	−1.1	−16.8	5.6	0.1
twinned	{1 0 −2}	0.0	−12.9	7.5	—
twinned	{1 0 2}	0.0	−14.8	6.0	—
twinned	{1 1 1}	−1.6	−16.8	5.2	—

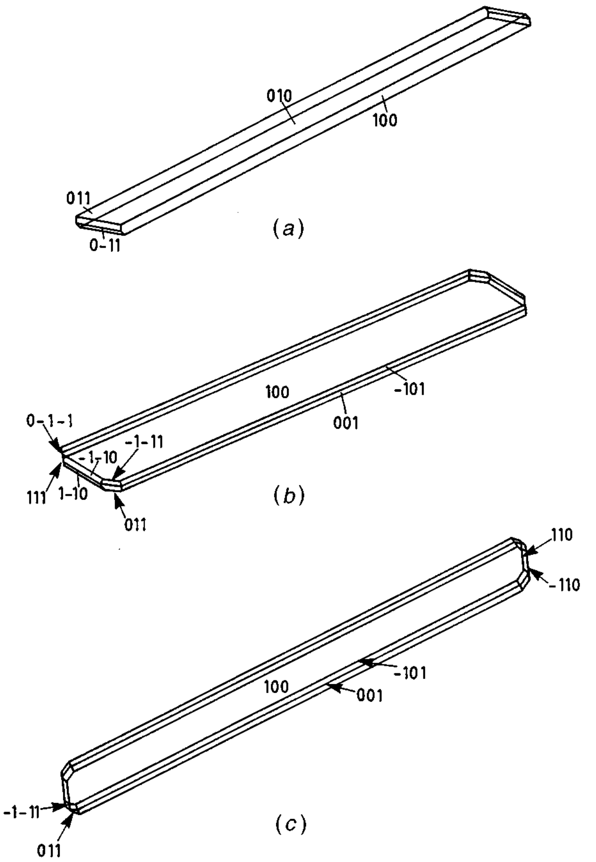

Fig. 5 (*a*) Predicted morphology of orthorhombic TNT and (*b*) predicted morphology of monoclinic phase of TNT; (*c*) predicted morphology of the twinned monoclinic phase

the slice and none contributing to bonding in the growth direction perpendicular to the {010} plane. In contrast to this, the small area of the {01 − 1} face is due to the presence of a strong network of intermolecular bonds of type O_a, O_c and O_d ($4O_a + O_c + O_d$) perpendicular to the {01 − 1} face.

The predicted faces of the monoclinic polymorph can be compared favourably with the experimentally determined morphologies of Gallagher and Sherwood.[20–22] They found that in general the faces {100}, {102}, {001}, {101}, {011}, {111} and {1 − 1 − 1} were observed for crystals grown from a variety of solvents, with {100} dominating. Variations in the crystal morphology were found with changes in supersaturation and solvent. Changes in the relative sizes of faces were observed and in some cases the {111} and {011} facets were absent. This phenomenon can be explained by the fact that there were only small differences in the attachment energies of the {102}, {011}, {110}, {1–1–1} and {111} faces. Crystals grown from methanol also exhibited the {10–2} and {20–3} faces, which can also be explained by the similarity of their attachment energies to those of the {102}, {011}, {110}, {1–1–1} and {111} faces.

The predicted morphology for the twinned monoclinic form is also very similar to those of the monoclinic polymorph. The intermolecular bonds T_a, T_b and T_d form a strong intermolecular bonding network perpendicular to the {110}, {1–1–1} and {011} faces causing rapid growth perpendicular to these faces and hence faces of small morphological importance, whilst all the principal intermolecular interactions contribute to bonding within the {100} face and none perpendicular to it, creating a very slow growing dominant {100} face.

Despite the agreement between predicted and observed crystallographic form being acceptable, the experimental crystal habits in general tend to be more prismatic when compared to theoretical simulations. The reasons for this are not clear at this time, but are likely to reflect the effect of the growth environmental factors such as solvent and supersaturation.

Conclusions

Previous experimental studies have indicated difficulties in obtaining consistent crystal forms of TNT. The calculations show that the difference in lattice energies between the two forms is quite small and that subtle differences can affect the form of the crystal and can cause twinning. The results indicate that such calculations can be of value in predicting crystal morphologies, with a plate-like morphology dominated by the {100} face predicted for the monoclinic form and a plate-like morphology dominated by the {010} face predicted for the orthorhombic form. Thus, for an energetic material such as TNT which can be experimentally difficult to study, computational modelling can provide a useful tool to aid understanding, and in potentially controlling the properties such as crystal form and morphology for TNT.

Further work is currently in hand to assess the role of growth environmental factors with a view to rationalising discrepancies between the morphological simulations and the experimentally observed crystal morphology.

The authors would like to acknowledge J. R. C. Duke of PERME, Waltham Abbey, Essex, for allowing access to his fractional coordinates of the monoclinic and orthorhombic polymorphs of 2,4,6-trinitrotoluene prior to publication. The involvement of R. Docherty and G. Clydesdale in the early stages of this work is also gratefully acknowledged. K. J. R. also acknowledges the Engineering and Physical Sciences Research Council (UK) for the current support of a senior fellowship.

References

1 J. A. R. P. Sarma and G. R. Desiraju, *J. Chem. Soc., Perkin Trans. 2*, 1987, 1187.
2 W. Jones, C. R. Theocharis, J. M. Thomas and G. R. Desiraju, *J. Chem. Soc., Chem Commun.*, 1983, 1443.
3 M. C. Etter, R. B. Kress, J. Bernstein and D. J. Cash, *J. Am. Chem Soc.*, 1984, **106**, 6921.
4 A. Gavezzotti and G. Filippini, *J. Am. Chem. Soc.*, 1995, **117**, 12299.
5 V. Benghiat and L. Leiserowitz, *J. Chem. Soc.*, 1972, 1763.
6 J. D. Dunitz and J. Bernstein, *Acc. Chem. Res.*, 1995, **28**, 193.
7 G. Desiraju, *Crystal Engineering, the Design of Organic Solids*, *Mater. Sci. Monogr.*, 54, Elsevier, Amsterdam, 1989.
8 L. A. Errede, M. C. Etter, R. C. Williams and S. M. Darnauer, *J. Chem. Soc., Perkin Trans. 2*, 1981, 233.
9 J. Bernstein, I. Bar and A. Christensen, *Acta Crystallogr., Sect. B*, 1976, **32**, 1609.
10 I. Bar and J. Bernstein, *Acta Crystallogr., Sect. B*, 1977, **33**, 1738.
11 I. Bar and J. Bernstein, *Acta Crystallogr., Sect. B*, 1982, **38**, 121.
12 J. Bernstein, M. Engel and A. T. Hagler, *J. Chem. Phys.*, 1981, **75**, 2346.
13 L. A. Burkardt and J. H. Bryden, *Acta Crystallogr.*, 1954, **1**, 135.
14 J. R. C. Duke, 1981, unpublished work.
15 P. Freidlander, *Z. Kristallogr.*, 1879, **3**, 169.
16 E. Hertel and G. Römer, *Z. Phys. Chem. B*, 1930, **2**, 77.
17 R. Hullgren, *J. Chem. Phys.*, 1936, **4**, 84.
18 E. Artini, *R. C. Acad. Lincei*, 1915, **24**, 274.
19 W. C. McCrone, *Anal. Chem.*, 1949, **21**, 1583.
20 H. G. Gallagher and J. N. Sherwood, *The Influence of Lattice Imperfections on the Chemical Reactivity of Solids: The Growth and Purification of TNT Single Crystals.*, Avail. NTVS. Gov. Rep. Announce. Index (NS), 1984, **84**, 83.
21 H. G. Gallagher and J. N. Sherwood, *The Growth and Purification of Single Crystals of TNT*, *Mater. Res. Soc. Symp. Proc.*, 1993, **296**, 215.
22 H. G. Gallagher and J. N. Sherwood, *J. Chem. Soc., Faraday Trans.*, 1996, **92**, 2107.
23 P. Bladon and R. Breckinridge, INTERCHEM, University of Strathclyde, UK, 1986.
24 R. Docherty, PhD Thesis, Strathclyde University, 1989.
25 R. Buckingham and J. Corner, *Proc. R. Soc. London*, 1947, **189**, 118.
26 G. Nemethy, M. S. Pottle and H. A. Scheraga, *J. Phys. Chem.*, 1983, **87**, 1883.
27 M. J. S. Dewar, E. G. Zoebisch, E. F. Healy and J. J. P Stewart, *J. Am. Chem. Soc.*, 1985, **107**, 3902.
28 J. J. P. Stewart, *J Comput.-Aided Mol. Design*, 1990, **4**, 1.
29 G. Clydesdale, R. Docherty and K. J. Roberts, *Comput. Phys. Commun.*, 1991, **64**, 311.
30 G. Clydesdale, R. Docherty and K. J. Roberts, QCPE Program No. 670, Quantum Chemistry Program Exchange, Indiana University, Bloomington, Indiana, USA.
31 G. Clydesdale, R. Docherty and K. J. Roberts, *Proc. Conf. Crystal Growth Organic Materials*, ed. A. S. Myerson, D. A. Green and P. Meenen Washington, DC, 1995; *J. Crystal Growth*, 1996, **166**, 78.
32 F. A. Momany, R. F. McGuire, A. W. Burgess and H. A. Scheraga, *J. Phys. Chem.*, 1975, **79**, 2361.
33 S. Lifson, A. T. Hagler and P. Dauber, *J. Am. Chem. Soc.*, 1979, **101**, 5111.
34 D. E. Williams, *J. Chem. Phys.*, 1966, **45**, 3370.
35 A. Bravais, *Etudes Crystallographiques*, Paris, 1913.
36 G. Freidel, *Bull. Soc. Fr. Mineral.*, 1907, **30**, 326.
37 J. D. H. Donnay and D. Harker, *Am. Mineral.*, 1937, **22**, 463.
38 J. R. Holden, C. Dickinson and C. M. Bock, *J. Phys. Chem.*, 1972, **76**, 3597.
39 C. Dickinson, J. M. Stewart and J. R. Holden, *Acta Crystallogr.*, 1966, **21**, 663.
40 W. R. Carper, L. P. Davis and M. W. Extine, *J. Phys. Chem.*, 1982, **86**, 459.
41 G. Edwards, *Trans. Faraday Soc.*, 1950, **46**, 423.
42 C. Lenchitz and R. W. Velidly, *J. Chem. Eng. Data*, 1920, **15**, 3, 401.
43 D. G. Graber, F. C. Rauch and A. J. Fanelli, *J. Phys. Chem.*, 1969, **73**, 3514.

Paper 6/03983I; *Received* 6th *June*, 1996